

## Multimode instabilities in a homogeneously broadened ring laser

L. A. Lugiato

*Dipartimento di Fisica dell'Università degli Studi di Milano, via Celoria 16, I-20133 Milano, Italy*

L. M. Narducci and E. V. Eschenazi

*Department of Physics, Drexel University, Philadelphia, Pennsylvania 19104*

D. K. Bandy and N. B. Abraham

*Department of Physics, Bryn Mawr College, Bryn Mawr, Pennsylvania 19010*

(Received 21 February 1985)

This paper contains a description of the behavior of a multimode unidirectional ring laser with a homogeneously broadened active medium. Our formulation is based on the conventional Maxwell-Bloch (MB) equations, but is distinguished from other treatments by the inclusion of a finite mirror reflectivity and an arbitrary value of the gain parameter. We review the steady-state behavior of the system and analyze the longitudinal profile of the field and of the atomic variables. With an appropriate transformation of variables, we transform the boundary conditions of the ring cavity into standard periodicity type, even in the presence of a finite reflectivity, and derive an infinite hierarchy of coupled mode equations. We analyze exactly the linear stability of the system, and investigate the dependence of the instability domain on the reflectivity and gain parameters. A numerical study of the full MB equations for a parameter range of the type explored in the recent experiments by Hillman *et al.* [Phys. Rev. Lett. 52, 1605 (1984)] reveals similarities, but also considerable differences between the results of the theory and the main experimental signatures of their instability. However, the injection of numerical noise shows the presence of numerous coexisting basins of attraction which are likely to play a significant role in the dynamics of a noisy laser.

### I. INTRODUCTION

The occurrence of sustained spontaneous oscillations is a well-established phenomenon that affects nearly every type of laser under appropriate operating conditions.<sup>1</sup> Models of homogeneously broadened active media have played a leading theoretical role in the study of instabilities since the early 1960s;<sup>2</sup> in fact, criteria for the emergence of self-pulsing in single-mode homogeneously broadened systems were advanced, even before the discovery of the ruby laser,<sup>3</sup> and were then generalized to multimode operation around 1968.<sup>4</sup>

The behavior of single-mode lasers has been analyzed extensively over the last decade, especially over the range of parameters where the laser equations develop an instability<sup>5</sup> of the type discovered by Lorenz<sup>6</sup> in his well-known studies of convective hydrodynamic instabilities. Multimode systems have received comparably more limited attention from the viewpoint of their stability properties after the early studies of Risken and Nummedal, and of Graham and Haken, apart from the recent investigations of ultrashort pulses by Haken and Ohno.<sup>7</sup>

The behavior of these systems in the linearized regime around their steady state is well understood.<sup>8</sup> The amplitude of the single-mode laser becomes unstable in the so-called "bad-cavity" limit if the linewidth  $\kappa$  of the only excited cavity mode exceeds the sum of the polarization ( $\gamma_{\perp}$ ) and population ( $\gamma_{\parallel}$ ) relaxation rates and if the laser gain is larger than a certain threshold value. When the cavity linewidth is smaller than  $\gamma_{\perp} + \gamma_{\parallel}$ , the resonant mode is al-

ways stable for arbitrary values of the gain parameter. Nonresonant modes, however, can become unstable if the unsaturated gain is sufficiently large and the intermode spacing is small enough.

A common feature of the type of instabilities displayed by homogeneously broadened lasers is the high value of the self-pulsing threshold (often called the second threshold) which is typically some ten times higher than the ordinary threshold for laser action, when measured in terms of the unsaturated gain parameter.

Yet, a recent experiment (Hillman *et al.*)<sup>9</sup> demonstrated the existence of a spectacular instability not far above the ordinary laser threshold in a cw-pumped dye laser operating in the "good-cavity" limit. This instability is characterized by a discontinuous increase of the average dye laser output power, the sudden emergence of symmetric sidebands, and the simultaneous disappearance of the laser resonant spectral component. Seemingly, the only unusual features of the experimental setup are the very high reflectivity of the mirrors in the ring cavity and the extremely large number of cavity modes under the gain profile of the active medium. In spite of the fairly typical arrangement, the observed behavior is difficult to explain in terms of our current understanding of the Risken-Nummedal and Graham-Haken models for at least two reasons: First, the dye laser gain required to trigger this effect is only slightly larger than what is required to produce normal laser action and second, the resonant laser mode is apparently suppressed discontinuously by the emerging sidebands for increasing values of

the pump parameter. The Risken-Nummedal-Graham-Haken instability, instead, is characterized by a much higher second threshold and by the persistent presence of the central laser component.

In an attempt to shed some light onto these apparently conflicting observations, we have undertaken a detailed analysis of both the linearized behavior and the nonlinear evolution of a multimode laser. Most earlier studies of instabilities have assumed, more or less explicitly, that the unsaturated gain per pass and the mirror transmittivity  $T$  are sufficiently small to justify the assumption that the field is spatially uniform in steady state.<sup>10</sup> Here, we remove this restriction and allow the possibility that the laser may have mirrors with arbitrary reflectivity and an active medium with any value of the unsaturated gain.

We have discovered, nor surprisingly, that multimode lasers possess a rather complicated phenomenology that includes periodic and chaotic attractors, soft- and hard-mode instabilities, and even the appearance of square-wave pulsations for a high density of cavity modes. The existence of numerous coexisting attractors suggests that noise may play a significant role in prescribing the actual observable evolution. Unfortunately, at this point, we are still unable to identify all the main signatures of the Hillman *et al.* instability in our numerical results.

The paper is organized as follows. In Sec. II we review the steady-state behavior of a homogeneously broadened laser with special attention to the role played by the finite reflectivity of the mirrors and the arbitrary gain (i.e., away from the mean-field limit). In Sec. III we derive an infinite hierarchy of coupled-mode equations; we study the steady-state configuration of a truncated five-mode system and demonstrate the possibility of discontinuous turn on and hysteric behavior in such solutions. In Sec. IV we carry out a linear stability analysis of the Maxwell-Bloch (MB) equations and derive a new characteristic equation for the eigenvalues that generalizes the well-known results of Ref. 4. In Sec. V we explore the dynamical evolution of selected multimode unstable systems with varying values of the cavity intermode separation. Depending on the chosen parameters we identify periodic and irregular oscillations, square-wave pulsing, and isolated attractors which are reminiscent of the five-mode solution discussed in Sec. III. The power spectra of the output field modulus display sharp lines and broadband features which can be readily correlated with the shape of the time-dependent pulsations. Finally, in Sec. VI we summarize our findings and provide a critical comparison between the numerical solutions, and the results of the measurements by Hillman *et al.*

## II. MAXWELL-BLOCH EQUATIONS: STEADY-STATE CONSIDERATIONS

We consider the behavior of a traveling-wave field interacting with a homogeneously broadened laser medium in a unidirectional ring cavity. As in many earlier studies of this problem, we model the active medium as a collection of homogeneously broadened two-level atoms with a transition frequency  $\omega_A$  between the lasing levels, and relaxation rates  $\gamma_{\perp}$  and  $\gamma_{\parallel}$  for the polarization and popula-

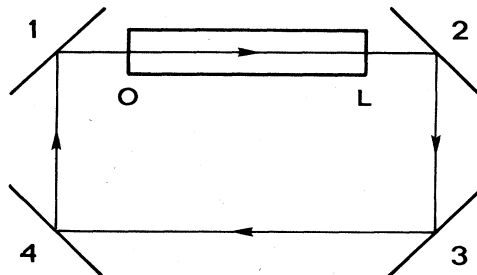


FIG. 1. Schematic representation of the unidirectional ring resonator. Mirrors 1 and 2 have an arbitrary reflectivity coefficient  $R$ , while mirrors 3 and 4 are perfect reflectors. The active medium is confined to the longitudinal region  $0 < z < L$ .

tion difference, respectively. The cavity is shaped as a ring resonator which can only support propagation along a single direction (Fig. 1). In our development the mirrors are allowed to have an arbitrary reflectivity and the unsaturated gain parameter per pass is not limited to small values, in spite of the fact that the removal of these restrictions causes the cavity field to acquire a nonuniform longitudinal profile. Transverse effects, however, are ignored throughout, by enforcing the plane-wave approximation.

The basic equations of motion are the well-known MB equations

$$\frac{\partial \mathcal{F}}{\partial z} + \frac{1}{c} \frac{\partial \mathcal{F}}{\partial t} = -\alpha \mathcal{P}, \quad (2.1a)$$

$$\frac{\partial \mathcal{P}}{\partial t} = \gamma_{\perp} [\mathcal{F} \mathcal{D} - (1 + i\tilde{\Delta}) \mathcal{P}], \quad (2.1b)$$

$$\frac{\partial \mathcal{D}}{\partial t} = -\gamma_{\parallel} \left[ \frac{1}{2} (\mathcal{F}^* \mathcal{P} + \mathcal{F} \mathcal{P}^*) + \mathcal{D} + 1 \right], \quad (2.1c)$$

for the complex field envelope  $\mathcal{F}$ , the atomic polarization envelope  $\mathcal{P}$ , and the population difference  $\mathcal{D}$ ;  $\alpha$  represents the small signal gain constant per unit length, and  $\tilde{\Delta} = (\omega_A - \omega_L) / \gamma_{\perp}$  is the scaled detuning between the atomic and the (unknown) laser frequencies. Equations (2.1a)–(2.1c) must be supplemented by the boundary conditions

$$\mathcal{F}(0, t) = R \mathcal{F}(L, t - \Delta t) e^{-i\delta_0}, \quad (2.2)$$

where  $\Delta t = (\mathcal{L} - L) / c$ ;  $\mathcal{L}$  is the length of the ring resonator,  $L$  is the length of the active medium, and  $\delta_0$  is the accumulated phase difference per round trip [ $\delta_0 = (L/c)(\omega_C - \omega_L)$ ] due to a possible mismatch between a selected cavity resonance  $\omega_C$  and the field carrier frequency  $\omega_L$ .

Equations (2.1) can easily be solved in steady state as shown later in this section. Because, however, the resonator may have significant transmission losses, and the very notion of cavity mode as a stable resonating structure is not well defined under these conditions, an alternative version of the MB equations becomes preferable for the purpose of deriving an infinite hierarchy of coupled-mode equations.

For this purpose, we follow a procedure first proposed by Benza and Lugiato<sup>11</sup> and introduce the new indepen-

dent variables

$$\begin{aligned} z' &= z, \\ t' &= t + \frac{\mathcal{L} - L}{c} \frac{z}{L}, \end{aligned} \quad (2.3)$$

and the new dependent variables

$$F(z', t') = \mathcal{F}(z', t') \exp \left[ \frac{z'}{L} \ln(Re^{-i\delta_0}) \right], \quad (2.4a)$$

$$P(z', t') = \mathcal{P}(z', t') \exp \left[ \frac{z'}{L} \ln(Re^{-i\delta_0}) \right], \quad (2.4b)$$

$$D(z', t') = \mathcal{D}(z', t') \exp \left[ \frac{2z'}{L} \ln R \right]. \quad (2.4c)$$

The role of the transformation (2.3) is to remove the time delay from the boundary conditions in the new frame of reference; the transformation (2.4) eliminates the multiplicative factors that appear in Eq. (2.2), so that the new boundary conditions for the field amplitude  $F(z', t')$  become

$$F(0, t') = F(L, t'). \quad (2.5)$$

The new equations of motion take the form

$$\frac{\partial F}{\partial z'} + \frac{\mathcal{L}}{cL} \frac{\partial F}{\partial t'} = - \frac{|\ln R|}{L} F + i(\delta_{AC} - \Delta) \frac{\mathcal{L}}{cL} F - \alpha P, \quad (2.6a)$$

$$\frac{\partial P}{\partial t'} = \gamma_{\perp} \left[ FD \exp \left[ \frac{2z'}{L} |\ln R| \right] - (1 + i\tilde{\Delta}) P \right], \quad (2.6b)$$

$$\frac{\partial D}{\partial t'} = -\gamma_{\parallel} \left[ \frac{1}{2}(FP^* + F^*P) + D + \exp \left[ -\frac{2z'}{L} |\ln R| \right] \right]. \quad (2.6c)$$

The price one has to pay in exchange for the simple boundary conditions (2.5) is the appearance of space-dependent factors in the equations of motion. This is, however, only a minor inconvenience, since the new set of partial differential equations and their boundary conditions allow a "natural" modal expansion of the ordinary Fourier type, as if the cavity had perfectly reflecting surfaces.

An additional advantage of the present formulation is that the new field amplitude  $F(z', t')$  usually displays small deviations from longitudinal uniformity, under steady-state conditions, even for relatively small values of the mirror reflectivity and large values of the unsaturated gain per pass. This fact is not obvious and will be justified by the following analysis.

In steady state, the MB equations (2.1) can be solved at once for the atomic parameters with the result

$$\mathcal{P}_{st}(z) = -\mathcal{F}_{st}(z) \frac{(1 - i\tilde{\Delta})}{1 + \tilde{\Delta}^2 + |\mathcal{F}_{st}(z)|^2}, \quad (2.7a)$$

$$\mathcal{D}_{st}(z) = -\frac{1 + \tilde{\Delta}^2}{1 + \tilde{\Delta}^2 + |\mathcal{F}_{st}(z)|^2}. \quad (2.7b)$$

The field equation then becomes

$$\frac{d}{dz} \mathcal{F}_{st}(z) = \frac{\alpha(1 - i\tilde{\Delta})}{1 + \tilde{\Delta}^2 + |\mathcal{F}_{st}(z)|^2} \mathcal{F}_{st}(z). \quad (2.8)$$

It is convenient to represent the complex field profile in the form  $\mathcal{F}_{st}(z) = \rho e^{i\theta}$ , where the modulus and phase satisfy the coupled equations

$$\frac{d\rho}{dz} = \frac{\alpha\rho}{1 + \tilde{\Delta}^2 + \rho^2}, \quad (2.9a)$$

$$\frac{d\theta}{dz} = -\frac{\alpha\tilde{\Delta}}{1 + \tilde{\Delta}^2 + \rho^2}. \quad (2.9b)$$

From the identity

$$\frac{1}{\rho} \frac{d\rho}{dz} = -\frac{1}{\tilde{\Delta}} \frac{d\theta}{dz} \quad (2.10)$$

we obtain

$$\ln \left[ \frac{\rho(z)}{\rho(0)} \right] = -\frac{1}{\tilde{\Delta}} [\theta(z) - \theta(0)], \quad (2.11)$$

while from Eq. (2.9a), we can derive a transcendental equation for  $\rho(z)$

$$(1 + \tilde{\Delta}^2) \ln \left[ \frac{\rho(z)}{\rho(0)} \right] + \frac{1}{2} [\rho^2(z) - \rho^2(0)] = \alpha z. \quad (2.12)$$

Finally, we express the steady-state boundary conditions (2.2) in terms of the field modulus and phase:

$$\rho(0) e^{i\theta(0)} = R\rho(L) e^{i\theta(L)} e^{-i\delta_0}. \quad (2.13)$$

Equation (2.13) combined with Eq. (2.11) (specialized at  $z=L$ ) yields the mode-pulling formula

$$\omega_L = \frac{\omega_c \gamma_{\perp} + \omega_A \kappa}{\kappa + \gamma_{\perp}} \quad (2.14)$$

or in terms of  $\tilde{\Delta}$ ,

$$\tilde{\Delta} = \frac{\tilde{\delta}_{AC}}{1 + \tilde{\kappa}}, \quad \tilde{\kappa} = \frac{c |\ln R|}{\mathcal{L} \gamma_{\perp}},$$

where  $\tilde{\kappa}$  is the scaled field damping rate out of the cavity. This result remains valid for arbitrary longitudinal field profiles. Equation (2.12) (for  $z=L$ ) and the boundary conditions (2.13) yield the relation

$$\rho^2(0) = \frac{2R^2}{1 - R^2} [\alpha L - (1 + \tilde{\Delta}^2) |\ln R|] \quad (2.15)$$

and the gain threshold condition

$$\alpha L \geq (1 + \tilde{\Delta}^2) |\ln R|.$$

The required field profile can be obtained from Eqs. (2.12) and (2.15) by elementary numerical methods. A few typical profiles are shown in Fig. 2(a). Evidently, for the chosen atomic and cavity parameters, the profile of the field  $\mathcal{F}$  deviates significantly from uniformity; on the other hand, the modulus of the new field amplitude  $F$  is very nearly constant over the entire active medium [Fig. 2(b)]. If, in the course of approximate calculations, it should be necessary to require spatial uniformity, the best

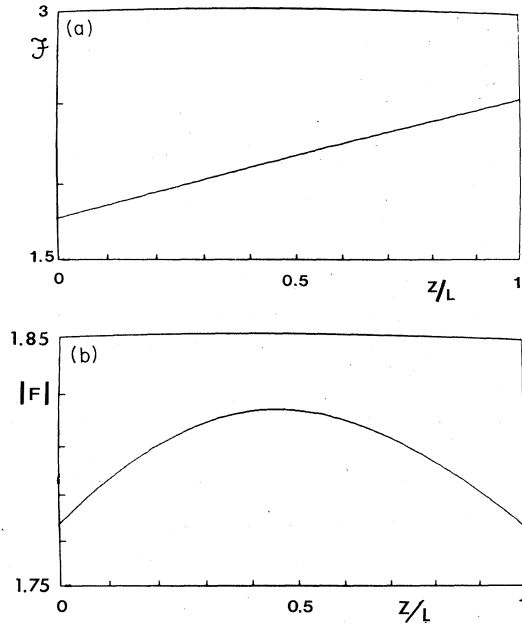


FIG. 2. (a) Longitudinal profile of the field amplitude  $|\mathcal{F}|$  as a function of the scaled coordinate  $z/L$ . The parameters used in this simulation are  $\alpha L=2$ ,  $R=0.7$ , mode spacing  $=5$ ,  $\omega_A=\omega_C$ . The derivation of  $|\mathcal{F}|$  from uniformity is 35%. (b) Same as (a) for  $|F|$  on a greatly expanded vertical scale; the derivation of  $|F|$  from uniformity is 2.5%.

strategy is to operate in the primed reference system (2.3) and in terms of the new field and atomic variables (2.4).

We observe, finally, that in the mean-field limit ( $\alpha L \rightarrow 0$ ,  $R \rightarrow 1$ , with  $\alpha L/T \equiv 2C = \text{const}$ ) the profile of the field  $\mathcal{F}$  (which becomes identical to that of  $F$ ) is uniform in space. In particular, from Eq. (2.15) the well-known result

$$|\mathcal{F}_{\text{st}}|^2 = 2C - (1 + \tilde{\Delta}^2) \quad (2.16)$$

follows at once.

### III. COUPLED-MODE EQUATIONS

For special applications, it is often convenient to replace the MB equations with a suitable infinite set of coupled ordinary differential equations to be truncated according to appropriate criteria. As already mentioned, the best starting point for a modal decomposition is the set of equations (2.6) because of the convenient form of the boundary conditions for the field variable  $F(z', t')$ . In fact, the Fourier representation of the field and atomic variables

$$\begin{pmatrix} F(z', t') \\ P(z', t') \\ D(z', t') \end{pmatrix} = \sum_{n=-\infty}^{+\infty} e^{ik_n z'} \begin{pmatrix} f_n(t') \\ p_n(t') \\ d_n(t') \end{pmatrix} \quad (3.1)$$

is automatically consistent with Eq. (2.5) provided we select the wave numbers  $k_n$  equal to integer multiples of  $2\pi/L$ . ( $k_n = 2\pi/L$ ,  $n=0, \pm 1, \pm 2, \dots$ ) Modal expansions of this type have been used frequently in laser phys-

ics. Here, Eq. (3.1) acquires a special significance because it fits exactly the boundary conditions and thus allows the interpretation of the expansion coefficients  $f_n(t')$  as the electromagnetic mode amplitudes of the ring cavity in the new  $(z', t')$  frame. This is especially satisfactory because in the original coordinate system the notion of cavity modes would have been hard to support with any rigor because of the "leaky" nature of the resonator.

In Eq. (3.1) we have  $d_{-n}(t') = d_n^*(t')$  because of the real nature of the population variable. Over the range  $0 \leq z \leq L$ , the chosen modal functions form a complete, orthonormal basis set such that

$$\frac{1}{L} \int_0^L dz' e^{ik_n z'} e^{-ik_m z'} = \delta_{n,m}. \quad (3.2)$$

Upon substituting Eqs. (3.1) into the MB equations (2.6), and with the help of the orthonormality condition (3.2), we obtain the following coupled equations:

$$\frac{d}{d\tau} f_n = -i\tilde{\alpha}_n f_n - \tilde{\kappa} \left[ \left( 1 - i \frac{\tilde{\delta}_{AC} - \tilde{\Delta}}{\tilde{\kappa}} \right) f_n + 2C p_n \right], \quad (3.3a)$$

$$\frac{d}{d\tau} p_n = \sum_{m,l} f_m d_l \xi_{m,l,n} - (1 + i\tilde{\Delta}) p_n, \quad (3.3b)$$

$$\frac{d}{d\tau} d_n = -\tilde{\gamma} \left[ \frac{1}{2} \sum_m (f_m p_{m-n}^* + f_m^* p_{m+n}) + d_n + \eta_n \right], \quad (3.3c)$$

where the time derivatives are taken with respect to the scaled time variable  $\tau = \gamma_{\perp} t'$  and where

$$\tilde{\alpha}_n = \frac{2\pi n c}{\mathcal{L} \gamma_{\perp}}, \quad (3.4)$$

$$\begin{pmatrix} \tilde{\kappa} \\ \tilde{\delta}_{AC} \\ \tilde{\Delta} \end{pmatrix} = \frac{1}{\gamma_{\perp}} \begin{pmatrix} \kappa \\ \delta_{AC} \\ \Delta \end{pmatrix}.$$

The mode-mode coupling coefficients  $\xi_{m,l,n}$  and the population equilibrium values  $\eta_n$  are defined by

$$\xi_{m,l,n} = \frac{1-R^2}{R^2} \frac{1}{2 |\ln R| + 2\pi i(m+l-n)}, \quad (3.5)$$

$$\eta_n = \frac{1-R^2}{2 |\ln R| + 2\pi i n}. \quad (3.6)$$

Note that, in the mean-field limit, we have

$$\xi_{m,l,n} \rightarrow \delta_{m+l,n}, \quad (3.5')$$

$$\eta_n \rightarrow \delta_{n,0}, \quad (3.6')$$

and the modal equations reduce to the well-known form derived, for example, in Ref. 10.

Equations (3.3) are especially useful when it can be argued that a small number of modes are operating simultaneously. The one-mode approximation, for example, has been used extensively in the past to study the chaotic evolution of the field  $f_0(\tau)$  in the unstable regime.<sup>5,12</sup> The limit of validity of the truncated hierarchy, on the other

hand, remains an open question, at least for arbitrary values of the parameters. It is clear, however, that the accuracy of a solution obtained from the superposition of a limited number of modes is sensitive to the spacing between adjacent cavity eigenvalues. In particular, when  $\alpha_1$  is sufficiently larger than  $\gamma_1$ , one may expect that even a severely truncated set of modal equations should serve the purpose well. However, this is not always the case, as discussed in more detail in Sec. V.

We now turn our attention to an interesting kind of steady-state solution of the truncated expansion that suggests the possibility of discontinuous behavior in certain regimes of pulsed operation. We are interested in the existence of what could be labeled a *symmetric solution* under resonant conditions  $\tilde{\delta}_{AC}=0$ , hence  $\tilde{\Delta}=0$ . By symmetric solutions we mean that the resonant field  $f_0$  has been suppressed to be exactly zero, that the field  $F(z', t')$  and polarization  $P(z', t')$  remain real, i.e.,

$$f_n = f_{-n}^*, \quad p_n = p_{-n}^*,$$

and that the Fourier amplitudes take the form ( $l=0, \pm 1, \pm 2, \dots$ ,  $\bar{n}$  a fixed index different from zero)

$$\begin{aligned} f_{2l\bar{n}} &= p_{2l\bar{n}} = 0, \\ f_{(2l+1)\bar{n}} &= \bar{f}_{(2l+1)\bar{n}} e^{-i(2l+1)v t}, \\ p_{(2l+1)\bar{n}} &= \bar{p}_{(2l+1)\bar{n}} e^{-i(2l+1)v t}, \\ d_{2l\bar{n}} &= \bar{d}_{2l\bar{n}} e^{-i2lv t}, \quad d_{(2l+1)\bar{n}} = 0, \end{aligned} \quad (3.7)$$

where the symbols  $\bar{f}$ ,  $\bar{p}$ , and  $\bar{d}$  denote constant values; all other modal amplitudes are equal to zero for any selected integer value  $\bar{n}$ . The oscillation frequency  $v$  is unknown, *a priori*, and must be calculated. The main reason for discussing a solution of this type is the existence of certain signatures which are also typical of the pulsations observed in the experiments by Hillman *et al.* Thus, for example, the conditions (3.7a) ensure that the resonant component will never be part of the total output field. Apparently, a symmetric solution is inconsistent with the exact modal equations (3.3), but it becomes consistent with them in the mean-field limit, a condition that appears to be well verified in the experiments by Hillman *et al.* In fact, in this case, a solution of the type

$$\begin{aligned} f_0 &= 0, \\ f_n &= 0, \quad |n| < \bar{n} \\ f_{\bar{n}}(t) &= \text{const} \times \exp(-i v t) \neq 0, \\ f_{-\bar{n}} &= f_{\bar{n}}^* \end{aligned}$$

implies that also the amplitudes  $f_{(2l+1)\bar{n}}$ ,  $p_{(2l+1)\bar{n}}$ ,  $d_{(2l)\bar{n}}$  are different from zero as a result of the structure of the modal equations. Because an exact analytic solution of this type is probably unfeasible, we consider explicitly a five-mode model (i.e.,  $n=0, \pm\bar{n}, \pm 2\bar{n}$ , for any integer  $\bar{n}$ ) in the limit  $R \rightarrow 1$ ,  $\alpha L \rightarrow 0$ , with  $2C \equiv \alpha L / T < \infty$ . We stress that infinitely many symmetric solutions (for  $\bar{n}=1, 2, \dots$ ) exist within the confines of the five-mode truncation. [Note, in addition, that the numerical results discussed in Sec. V give strong support to the conjecture

that the symmetric solutions (3.7) do indeed satisfy the entire infinite hierarchy of modal equations in the mean-field limit.]

The relevant equations of motion are

$$\frac{d}{d\tau} f_{\bar{n}} = i\tilde{\alpha}_{\bar{n}} f_{\bar{n}} - \tilde{\kappa}(f_{\bar{n}} + 2Cp_{\bar{n}}), \quad (3.8a)$$

$$\frac{d}{d\tau} p_{\bar{n}} = f_{\bar{n}} d_0 + f_{\bar{n}}^* d_{2\bar{n}} - p_{\bar{n}}, \quad (3.8b)$$

$$\frac{d}{d\tau} d_0 = -\tilde{\gamma}(f_{\bar{n}} p_{\bar{n}}^* + f_{\bar{n}}^* p_{\bar{n}} + d_0 + 1), \quad (3.8c)$$

$$\frac{d}{d\tau} d_{2\bar{n}} = -\tilde{\gamma}(f_{\bar{n}} p_{\bar{n}} + d_{2\bar{n}}). \quad (3.8d)$$

The five-mode truncation shows that the field modes are coupled not only by a slowly varying gain term ( $d_0$ ), but also by a component ( $d_{2\bar{n}}$ ) that oscillates at the beat frequency between the modes. This additional coupling is the "population pulsation term" identified, for example, in Ref. 13.

As shown in the Appendix, the amplitude and the oscillation frequency of the only nonzero mode in steady state are given by the coupled equations

$$1 = \frac{2C}{B} (1 + 4v_{\parallel}^2 + |f_{\bar{n}}|^2), \quad (3.9a)$$

$$v_1 - \tilde{\alpha} = \tilde{\kappa} \frac{v_1(1 + 4v_{\parallel}^2) - 2v_{\parallel}|f_{\bar{n}}|^2}{1 + 4v_{\parallel}^2 + |f_{\bar{n}}|^2}, \quad (3.9b)$$

$$\begin{aligned} B &= 3|f_{\bar{n}}|^4 + 4|f_{\bar{n}}|^2(1 - v_1 v_{\parallel} + 2v_{\parallel}^2) \\ &\quad + (1 + v_{\perp}^2)(1 + 4v_{\parallel}^2). \end{aligned} \quad (3.10)$$

In the good-cavity limit ( $\tilde{\kappa} \ll 1$ ) the operating frequency  $v_1$  is essentially  $\tilde{\alpha}_{\bar{n}}$  to within corrections of order  $\tilde{\kappa}$ , while the field intensity  $|f_{\bar{n}}|^2$  is a solution of the quadratic equation that results from Eq. (3.9a). It is a trivial matter to verify that a plot of  $|f_{\bar{n}}|^2$  as a function of  $C$  is double valued if

$$\tilde{\alpha}_{\bar{n}}^2 > \frac{3}{1 + \frac{4}{\tilde{\gamma}} \left[ 1 - \frac{2}{\tilde{\gamma}} \right]} \quad (3.11)$$

provided, of course,  $\tilde{\gamma} > 2(\sqrt{3} - 1) = 1.46$  in order to ensure that  $\tilde{\alpha}_{\bar{n}}^2$  is positive. A typical curve displaying the steady-state intensity as a function of the parameter  $C$  is shown in Fig. 3.

Assuming that a symmetric solution can be excited, the double valuedness of the steady state suggests that the turnon and turnoff of this solution may be discontinuous. Actually, numerical simulations based on the truncated set of equations (3.8) indicate that the symmetric solution does not bifurcate from the stationary state of the five-mode model given by  $|f_0|^2 = 2C - 1$ ,  $d_0 = -1/2C$ ,  $p_0 = f_0 d_0$ ; it does, however, have a stable domain of existence which is accessible by hard excitation. Once trapped in this domain, the five-mode solution indeed conforms to the requirements (3.7) and, in particular, displays the expected sudden turnoff, upon decreasing the gain parameter  $C$ .

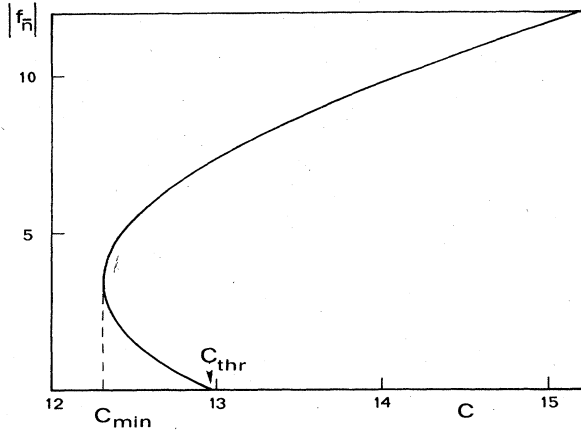


FIG. 3. Typical steady-state output intensity curve as a function of the gain  $C$  for values of the parameters leading to double-valued behavior;  $\bar{\alpha}_1 = 5$ ,  $\bar{\gamma} = 2$ .

An extension of this steady-state analysis to a larger number of modes involves very cumbersome algebraic manipulations and has not been pursued. Unfortunately, the relevance of this solution to the observed Hillman instability is only tenuous because, by construction, the beat frequency between the excited sidebands ( $2\alpha_{\bar{n}}$ , in the five-mode case) is independent of the gain and, in addition, the existence of discontinuities in the state equation is constrained by the inequality (3.11) which may not be satisfied in the Hillman experiment where  $\bar{\gamma}$  is likely to be smaller than unity.

#### IV. LINEAR STABILITY ANALYSIS

In this section we investigate the conditions under which unstable behavior develops in the neighborhood of one of the possible steady states of the ring laser system. The procedure adopted in the following calculation is conceptually identical to those of numerous earlier studies; the major difference arises from the spatial dependence of the field amplitude which is a consequence of the arbitrary gain and reflectivity parameters. This calculation is limited, at present, to the resonant case ( $\bar{\delta}_{AC} = 0$ ) and is constrained by the assumption that the fluctuations of the variables are real. This removes the possibility of describing possible phase instabilities. Because, however, small phase fluctuations in resonance do not grow in the mean-field limit, it is reasonable to expect that this condition will persist, for reasons of continuity, even when  $\alpha L$  or the transmittivity are no longer very small.

The linearized equations of motion that follow from Eqs. (2.1) are

$$\frac{\partial}{\partial z} \delta \mathcal{F} + \frac{1}{c} \frac{\partial}{\partial t} \delta \mathcal{F} = -\alpha \delta \mathcal{P}, \quad (4.1a)$$

$$\frac{\partial}{\partial t} \delta \mathcal{P} = \gamma_{\perp} (\delta \mathcal{F} \mathcal{D}_{st} + \mathcal{F}_{st} \delta \mathcal{D} - \delta \mathcal{P}), \quad (4.1b)$$

$$\frac{\partial}{\partial t} \delta \mathcal{D} = -\gamma_{\parallel} (\delta \mathcal{F} \mathcal{P}_{st} + \mathcal{F}_{st} \delta \mathcal{P} + \delta \mathcal{D}), \quad (4.1c)$$

where we have assumed  $\delta \mathcal{F} = \delta \mathcal{F}^*$  and  $\delta \mathcal{P} = \delta \mathcal{P}^*$ . We seek solutions of the type

$$\begin{pmatrix} \delta \mathcal{F}(z, t) \\ \delta \mathcal{P}(z, t) \\ \delta \mathcal{D}(z, t) \end{pmatrix} = e^{\lambda t} \begin{pmatrix} \delta f(z) \\ \delta p(z) \\ \delta d(z) \end{pmatrix} \quad (4.2)$$

and obtain the following expression for the polarization fluctuation  $\delta p(z)$ :

$$\delta p(z) = \frac{\gamma_{\perp}}{1 + \mathcal{F}_{st}^2} \frac{(\lambda + \gamma_{\parallel}) - \gamma_{\parallel} \mathcal{F}_{st}^2(z)}{(\lambda + \gamma_{\perp})(\lambda + \gamma_{\parallel}) + \gamma_{\perp} \gamma_{\parallel} \mathcal{F}_{st}^2(z)} \delta f(z). \quad (4.3)$$

Note that the reference phase of the steady-state field has been set equal to zero in eq. (4.3). On combining Eqs. (4.1a), (4.2), and (4.3), we obtain the field fluctuation equation

$$\frac{d}{dz} \delta f(z) = H(z) \delta f(z), \quad (4.4)$$

where

$$H(z) = -\frac{\lambda}{c} + \frac{\alpha \gamma_{\perp}}{1 + \mathcal{F}_{st}^2(z)} \frac{(\lambda + \gamma_{\parallel}) - \gamma_{\perp} \mathcal{F}_{st}^2(z)}{(\lambda + \gamma_{\perp})(\lambda + \gamma_{\parallel}) + \gamma_{\perp} \gamma_{\parallel} \mathcal{F}_{st}^2(z)}. \quad (4.5)$$

The formal solution of Eq. (4.4), of course, can be obtained trivially with the result

$$\delta f(z) = \delta f(0) \exp \left[ \int_0^z dz' H(z') \right] \equiv \delta f(0) e^{\psi(z)}. \quad (4.6)$$

The evaluation of the spatial integral can be carried out with a clever change of independent variables from  $z$  to  $\mathcal{F}_{st}(z)$  as done by Carmichael in the case of absorptive multimode optical bistability<sup>14</sup> and with the help of the field equation in steady state [Eq. (2.8)]. The result is

$$\begin{aligned} \psi(z) = & -\frac{\lambda z}{c} \\ & + \gamma_{\perp} \int_{\mathcal{F}_{st}(0)}^{\mathcal{F}_{st}(z)} d\mathcal{F}_{st} \\ & \times \frac{\lambda + \gamma_{\parallel} - \gamma_{\parallel} \mathcal{F}_{st}^2}{\mathcal{F}_{st} [(\lambda + \gamma_{\perp})(\lambda + \gamma_{\parallel}) + \gamma_{\perp} \gamma_{\parallel} \mathcal{F}_{st}^2]}. \end{aligned} \quad (4.7)$$

The integral in Eq. (4.7) can now be performed by elementary techniques. Thus, the required field fluctuation takes the form

$$\delta \mathcal{F}(z, t) = e^{\lambda t} \delta f(0) e^{\psi(z)}. \quad (4.8)$$

The boundary conditions

$$\delta \mathcal{F}(0, t) = R \delta \mathcal{F}(L, t - (\mathcal{L} - L)/c) \quad (4.9)$$

together with Eqs. (4.8) and (4.7) yield the following transcendental equation for the rate  $\lambda$ :

$$\lambda_n = -i\alpha_n - \frac{c |\ln R|}{\mathcal{L}} \frac{\lambda}{\lambda + \gamma_\perp} - \frac{c}{\mathcal{L}} \frac{\lambda + 2\gamma_\perp}{2(\lambda + \gamma_\perp)} \times \ln \left[ \frac{(\lambda + \gamma_\perp)(\lambda + \gamma_\parallel) + \gamma_\perp \gamma_\parallel \mathcal{F}_{st}^2(L)}{(\lambda + \gamma_\perp)(\lambda + \gamma_\parallel) + R^2 \gamma_\perp \gamma_\parallel \mathcal{F}_{st}^2(L)} \right], \quad n=0, \pm 1, \pm 2, \dots \quad (4.10)$$

Before discussing some of the exact solutions of Eq. (4.10), we first consider its mean-field limit. Thus we assume  $\alpha L \rightarrow 0$  and  $T \rightarrow 0$  with an arbitrary value of the ratio  $2C = \alpha L / |\ln R| \simeq \alpha L / T$ . Under these conditions, Eq. (4.10) can be approximated by

$$\tilde{\lambda}_n = -i\tilde{\alpha}_n - \tilde{\kappa} \frac{\tilde{\lambda}_n(\tilde{\lambda}_n + \tilde{\gamma}) + 2\mathcal{F}_{st}^2 \tilde{\gamma}}{(\tilde{\lambda}_n + \tilde{\gamma})(\tilde{\lambda}_n + 1) + \tilde{\gamma} \mathcal{F}_{st}^2}, \quad (4.11)$$

where  $\mathcal{F}_{st}^2 = 2C - 1$  and where, for convenience, we have scaled all the relevant rates to  $\gamma_\perp$  (thus,  $\tilde{\lambda}_n = \lambda_n / \gamma_\perp$ , etc.). This is the well-known result of the Risken-Nummedal analysis whose conclusions can be summarized as follows.

(a) For finite values of  $\gamma_\parallel$  and  $\gamma_\perp$  or, more precisely, for  $\gamma_\parallel, \gamma_\perp = \mathcal{O}(T^n)$  with  $\tilde{\gamma} < \infty$ ,  $\tilde{\kappa}$  is of order  $T$ , so that Eq. (3.10) can be solved by an iterative perturbation technique to obtain the important eigenvalue (i.e., the one whose real part can become positive; for a detailed discussion concerning the "stable" roots, see Ref. 13). Thus, if we set

$$\tilde{\lambda}_n = \tilde{\lambda}_n^{(0)} + \tilde{\kappa} \lambda_n^{(1)}$$

we find

$$\tilde{\lambda}_n^{(0)} = -i\tilde{\alpha}_n, \quad (4.12a)$$

$$\lambda_n^{(1)} = - \frac{\tilde{\lambda}_n^{(0)}(\tilde{\lambda}_n^{(0)} + \tilde{\gamma}) + 2\mathcal{F}_{st}^2 \tilde{\gamma}}{(\tilde{\lambda}_n^{(0)} + \tilde{\gamma})(\tilde{\lambda}_n^{(0)} + 1) + \tilde{\gamma} \mathcal{F}_{st}^2}. \quad (4.12b)$$

Because the real part of the zeroth-order contribution is identically equal to zero, the stability of the  $n$ th mode is entirely controlled by the first-order contribution to the eigenvalue; the real part of this term is given explicitly by

$$\text{Re} \lambda_n^{(1)} = \frac{(\tilde{\alpha}_n^2 - 2\tilde{\gamma} \mathcal{F}_{st}^2)[(1 + \mathcal{F}_{st}^2) - \tilde{\alpha}_n^2] - \tilde{\alpha}_n^2 \tilde{\gamma}(1 + \tilde{\gamma})}{[\tilde{\gamma}(1 + \mathcal{F}_{st}^2) - \tilde{\alpha}_n^2]^2 + \tilde{\alpha}_n^2(1 + \tilde{\gamma})^2}. \quad (4.13)$$

$\text{Re} \lambda_n^{(1)}$  can take on positive values for modes characterized by a frequency offset  $\tilde{\alpha}_n$  such that

$$\tilde{\alpha}_n^4 - \tilde{\gamma}[3(2C - 1) - \tilde{\gamma}]\tilde{\alpha}_n^2 + 4C(2C - 1)\tilde{\gamma}^2 < 0. \quad (4.14)$$

Thus, for a fixed value of  $\tilde{\gamma}$  the domain of instability is defined by the inequality

$$\tilde{\alpha}_{\min} \leq \tilde{\alpha}_n \leq \tilde{\alpha}_{\max}, \quad (4.15)$$

where

$$\left. \begin{aligned} \tilde{\alpha}_{\max} \\ \tilde{\alpha}_{\min} \end{aligned} \right\} = \left[ \frac{\tilde{\gamma}}{2} \right]^{1/2} \left[ 3(2C - 1) \pm \tilde{\gamma}([3(2C - 1) - \tilde{\gamma}]^2 - 16C(2C - 1))^{1/2} \right]^{1/2}. \quad (4.16)$$

It is also easy to see that, in this case, the resonant mode ( $\tilde{\alpha} = 0$ ) will always be stable.

(b) If both  $\gamma_\parallel$  and  $\gamma_\perp$  are of order  $T$ , with  $\tilde{\gamma}$  finite, the perturbation expansion fails and Eq. (4.11) is handled best by ordinary numerical techniques. The significant difference between cases (a) and (b) is that in the latter the resonant mode can become unstable provided the following condition is satisfied:

$$(\tilde{\kappa} - \tilde{\gamma} - 1)F_{st}^2 > (\tilde{\kappa} + 1)(\tilde{\kappa} + \tilde{\gamma} + 1). \quad (4.17)$$

This condition can be achieved if one increases the pump parameter to a sufficiently high level, but only in the bad-cavity situation  $\tilde{\kappa} > \tilde{\gamma} + 1$ .

In general, the instability domains of the eigenvalues are not very sensitive to the deviations from the mean-field conditions. Figures 4(a) and 4(b) display sets of real parts of the eigenvalue that is responsible for the emer-

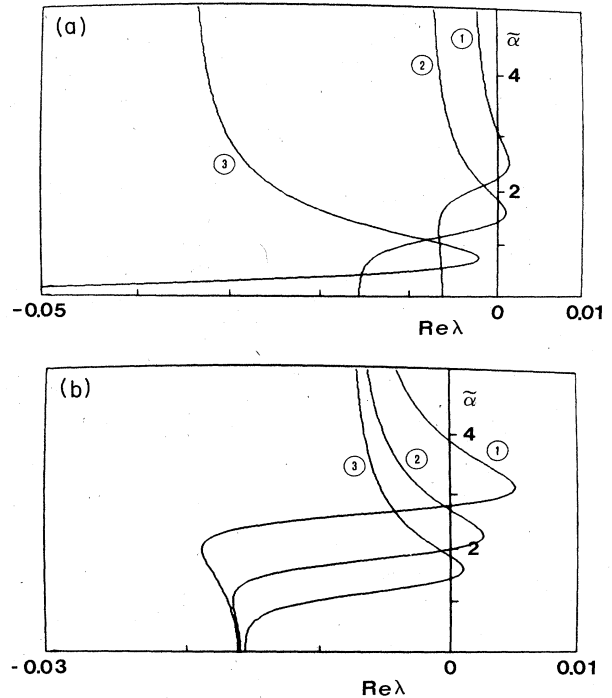


FIG. 4. (a) Behavior of the real part of the "unstable" eigenvalue for different values of the intermode spacing  $\tilde{\alpha}$  viewed as a continuous variable. The three curves refer to (1)  $R = 0.98$ , (2)  $R = 0.95$ , (3)  $R = 0.8$ . The common value of the gain parameter is  $\alpha L = 1$  and  $\tilde{\gamma} = 0.1$ . (b) Behavior of the real part of the unstable eigenvalues for different values of the intermode spacing  $\tilde{\alpha}$  viewed as a continuous variable. The three curves refer to (1)  $\alpha L = 4$ , (2)  $\alpha L = 2$ , (3)  $\alpha L = 1$ . The common value of the reflectivity is  $R = 0.95$  and  $\tilde{\gamma} = 0.1$ .

gence of unstable behavior. Figure 4(a) shows its dependence on the reflectivity, while Fig. 4(b) displays the effect of varying the small signal gain. A comparison of exact and approximate solutions obtained from Eqs. (4.10) and (4.11) is shown in Fig. 5. Clearly, even for rather large gain parameters and low reflectivity coefficients, the results do not display large differences.

### V. EVOLUTION OF A MULTIMODE LASER AND POWER SPECTRA OF THE OUTPUT FIELD

When dealing with cavity configurations where the mode spacing  $\tilde{\alpha}_1$  is of order unity or less, using the MB equations becomes almost unavoidable, particularly if the system is likely to develop instabilities. The numerical work of this section was carried out by solving the MB equations (2.6) in resonance ( $\delta_{AC}=0$ ) using the same integration scheme described in Ref. 4(b). For comparison, we have also solved several truncated versions of the modal expansion (3.3), also under resonance conditions, using a standard fourth-order Runge-Kutta routine. In both cases we have performed our calculations in double precision.

We divide our survey of the numerical results according to the values of the scaled cavity damping rate  $\tilde{\kappa}$ . Thus, in Sec. VA we discuss numerical simulations carried out in the good-cavity limit ( $\tilde{\kappa} \ll 1$ ), while in Sec. VB we analyze results pertaining to the bad-cavity configuration ( $\tilde{\kappa} > 1$ ).

#### A. The good-cavity limit

In the good-cavity limit, unstable bands of sidemodes may develop symmetrically on either side of line center; of course, a very different dynamic response can be expected, depending on the intermode spacing and on the total number of unstable modes. Note that according to the model discussed in Sec. II, the cavity damping rate  $\tilde{\kappa}$  and the intermode spacing  $\tilde{\alpha}_1$  are in a fixed relation with one another [ $\tilde{\kappa} = (|\ln R|/2\pi)\tilde{\alpha}_1$ ], so that for given values of the mirror reflectivity and cavity length  $\mathcal{L}$ ,  $\tilde{\kappa}$  is also fixed. On the other hand, real systems are likely to suffer non-negligible losses also from a variety of optical components besides the cavity mirrors. For this reason, we

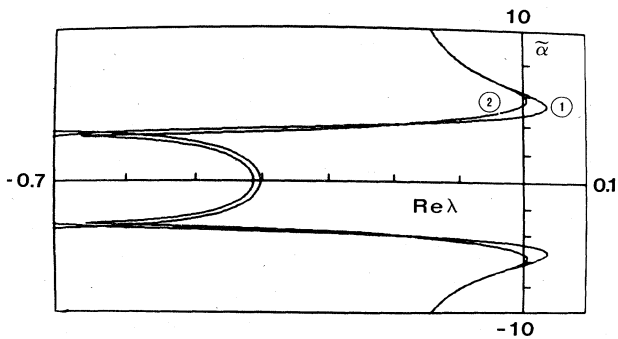


FIG. 5. Comparison between the real parts of the unstable eigenvalues obtained from the exact equation (4.10) and its mean-field limit (4.11). The parameters used in this simulation are  $\alpha L = 10$ ,  $R = 0.65$ , mode spacing  $= 3.0$ ,  $\tilde{\gamma} = 0.1$ .

may consider  $\tilde{\kappa}$  as an adjustable parameter and, if necessary, assign to it larger values than predicted on the basis of the formal definition  $c |\ln R| / \mathcal{L} \gamma_1$ .

If  $\tilde{\alpha}_1$  is sufficiently larger than unity, usually only one mode can be unstable during the linear evolution. In this case, as time progresses, one expects an essentially simple periodic behavior of the output intensity, apart from the unavoidable harmonic components introduced by the nonlinearities of the equations of motion. This is well confirmed by selected solutions of the MB equations with the system initially prepared in a state with a zero output field and polarization and a uniform inverted population. An example is shown in Figs. 6(a)–6(c). In this case, the parameters have been selected so that the very first sideband, at  $\tilde{\alpha}_1 = 5$ , falls within the instability domain [Fig. 6(a)]. The long-term behavior of the solution confirms, by inspection, that the period of the pulsations is indeed consistent with a radian frequency of 5 [Fig. 6(b)]; the power spectrum of the real output field envelope makes this precise [Fig. 6(c)]. Note that, as anticipated, several harmonic components with reasonable power levels are also observable.

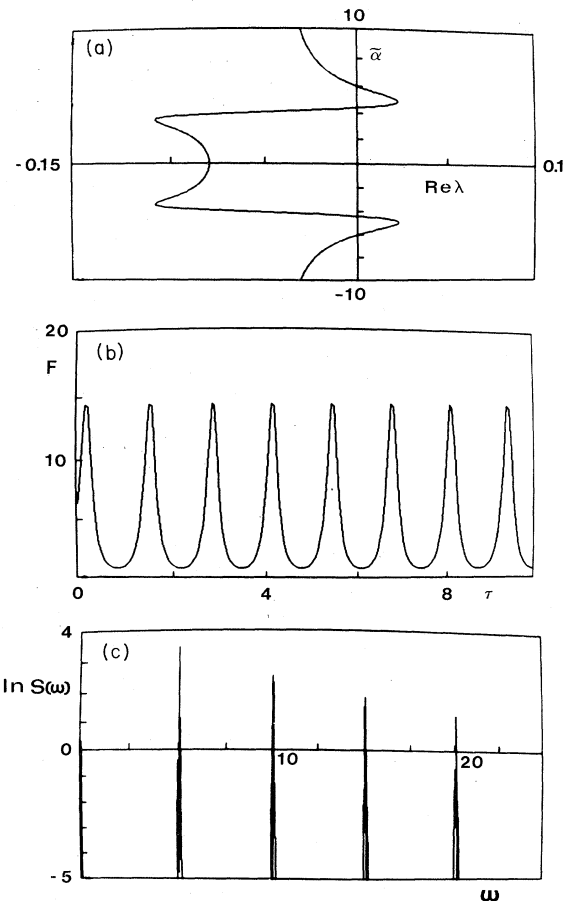


FIG. 6. (a) Real part of the unstable eigenvalue for different values of the intermode spacing  $\tilde{\alpha}$  viewed as a continuous variable. The parameters used in this study are  $\alpha L = 2$ ,  $R = 0.95$ ,  $\tilde{\gamma} = 0.5$ ,  $\tilde{\alpha}_1 = 5$ , and  $2C = 39$ . (b) Amplitude  $F(L, t)$  as a function of the scaled time  $\gamma_1 t$ . (c) Power spectrum of the output field on a semilogarithmic scale.

A second test is displayed in Figs. 7(a)–7(c). Here the parameters have been selected so that the second sideband at frequency  $\tilde{\alpha}_2=2$  falls within the instability region, while the first sideband is stable in the sense of linear stability. With the laser initially in a nonlasing state, the initial evolution of the output field displays a transient oscillatory pattern with a frequency of pulsations equal to  $\tilde{\alpha}_1$ . Gradually, however, a higher-frequency component develops [Fig. 7(a)] and eventually dominates [Fig. 7(b)]. This frequency is, in fact, equal to  $\tilde{\alpha}_2$  as confirmed by the power spectrum of the output field [Fig. 7(c)]. Note that the actual value of the fundamental frequency as measured from the power spectrum is not exactly equal to 2 because of frequency pulling effects. The correction, however, is of order  $\tilde{\kappa}=8.2 \times 10^{-3}$  and thus very small.

With such a limited number of harmonic components

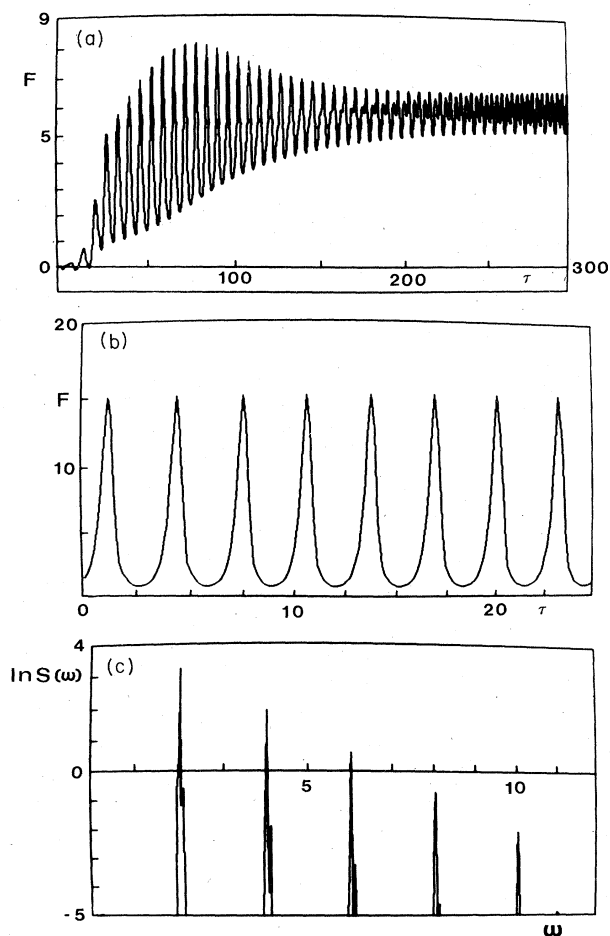


FIG. 7. (a) Amplitude  $F(L,t)$  as a function of the scaled time  $\gamma_1 t$  for  $\alpha L=2$ ,  $R=0.95$ ,  $\tilde{\gamma}=0.08$ ,  $\tilde{\alpha}_1=1$ , and  $2C=39$ . The initial conditions correspond to a state with zero field, zero polarization, and complete inversion. The frequency of oscillation is approximately equal to  $\tilde{\alpha}_1$  during the initial phase of the evolution; at later times, the field develops a modulation which eventually is the origin of a pulsation frequency equal to  $\tilde{\alpha}_2$  (the frequency of the unstable mode). (b) Long-time evolution of  $F(L,t)$ ; the frequency of pulsation of the field amplitude corresponds to  $\tilde{\alpha}_2$ . (c) Power spectrum of the output field on a semi-logarithmic scale.

in the exact solution, it is not unreasonable to expect that a five-mode truncation ( $n=0, \pm 1, \pm 2$ ) of the modal hierarchy should reproduce the basic features of the oscillations rather faithfully. Using the same initial conditions as in the previous case, an initial transient pulsation at frequency  $\tilde{\alpha}_1=1$  displays a gradual modulation that eventually dominates for long times. The long-term solution is exactly sinusoidal with a frequency  $\tilde{\alpha}_2=2$  and displays, of course, no harmonic components. The exact oscillation amplitude is reproduced, however, with a fairly large error ( $\approx 30\%$ ).

When the intermode spacing is considerably smaller than unity, entire bands of sidemodes can become unstable if the gain is sufficiently high. The evolution of the system, starting from an unstable stationary state of the MB equations, is characterized, at first, by a small amplitude oscillation with a frequency that corresponds rather closely to that of the unstable mode with the largest real part of the eigenvalue [Fig. 8(a)]. This is followed by a progressively more and more complicated amplitude modulation which is probably connected with the growth of additional unstable modes [Fig. 8(b)]. The fully grown pattern [Fig. 8(c)] displays very little in the way of apparent regularities except for a beat pattern at a frequency approximately equal to  $\tilde{\alpha}_1$ , probably because the relative phases of the individual modes undergo a slow temporal drift. The power spectrum is quite revealing, however. As shown in Fig. 8(d), the spectrum of the output field consists of a fundamental band of regularly spaced lines (the spacing between lines is equal to the selected intermode spacing) and its harmonic components. In addition, a narrower band of low-frequency beat notes is very prominent near the origin of the frequency axis.

The picture suggested by the spectrum of Fig. 8(d) is in qualitative agreement with Haken's suggestion<sup>8</sup> that the evolution is governed mainly by a packet of modes whose amplitude is a slowly varying function of space (as well as time, from the point of view of an observer at the exit port of the cavity), with an oscillation frequency roughly assigned by the most unstable mode and a frequency spread of the order of the instability range. A precise correlation between Haken's proposal and the type of behavior displayed in Fig. 8 will require additional analyses.

Matters are made more complicated by the presence of a chaotic attractor which appears at higher values of the gain [Figs. 9(a) and 9(b)] and by the tendency of high gain solutions to abandon the original oscillating pattern and to adopt a striking square-wave shape [Figs. 10(a) and 10(b)]; in the latter case the real field envelope has a much smaller average value than shown, for example, in Fig. 8, in closer qualitative agreement with the observed pulsations of the experiments by Hillman *et al.*, where the envelope of the oscillating field presumably has a zero average after the quenching of the resonant laser component. The frequency of these square waves, however, is  $\tilde{\alpha}_1$ —regardless of the Rabi frequency. These solutions are highly suggestive of the existence of additional neighboring attractors whose role in the overall picture is very much an open matter at this time.

The square-wave shapes obtained “spontaneously”

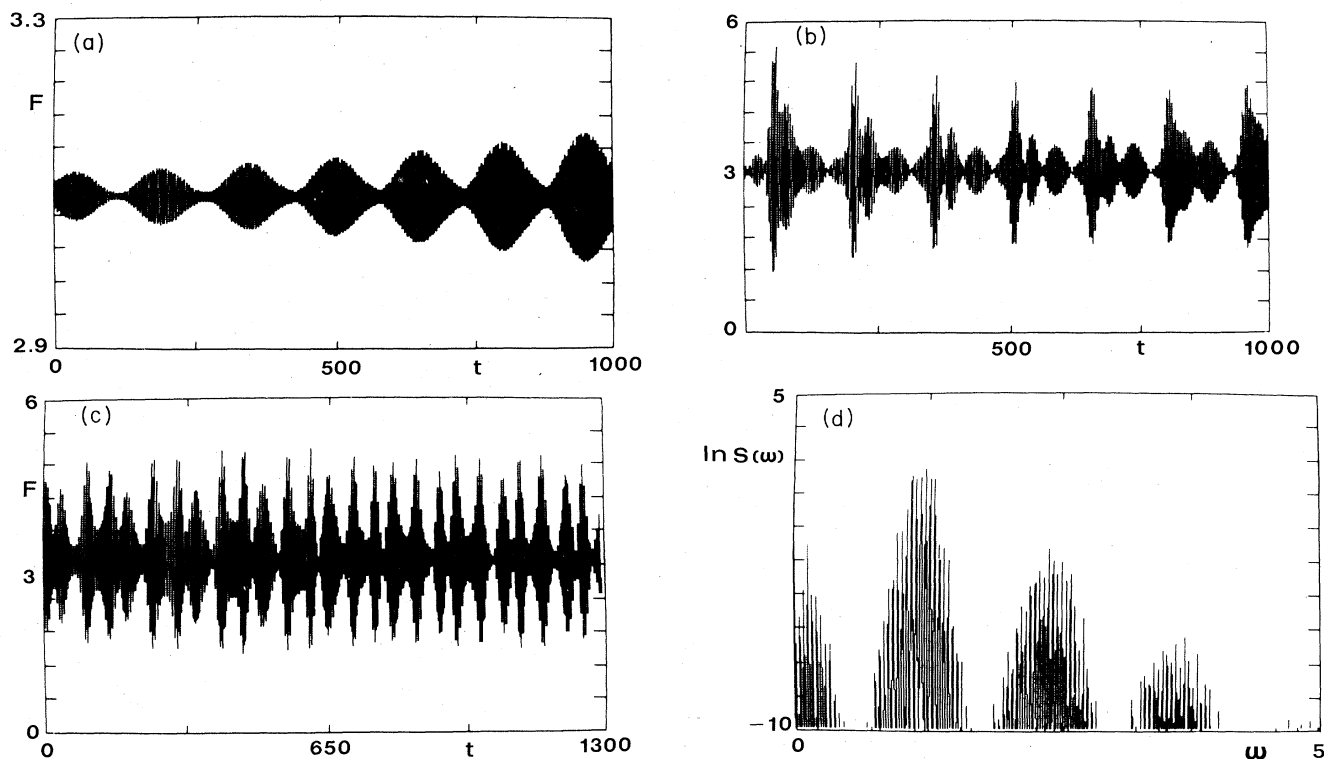


FIG. 8. First phase of the transient evolution of the field amplitude in a case when several of the sidebands are simultaneously unstable (in this case, three sidemodes on each side of  $\bar{\alpha}_n=0$  are unstable according to the linear stability analysis). The overall evolution from  $t=0$  to the end of (c) required many thousands of time units. In these figures the origin of the horizontal time axis is always reset to zero. The parameters used in this simulation are  $\alpha L=0.54$ ,  $R=0.95$ , mode spacing  $=0.05$ ,  $\bar{\gamma}=0.1$ . The cavity damping rate is set equal to 0.1 to accelerate the approach to steady state. Other simulations have been carried out with the theoretical value of  $\bar{\kappa}$  without appreciable differences in the final results. (b) A subsequent phase of the transient evolution of the field amplitude. The slowest modulation of the pattern corresponds to a frequency 0.04 which is approximately equal to the intermode spacing. (c) Fully developed oscillation pattern of the output field amplitude. (d) Power spectrum of the output field on a semilogarithmic scale.

under the influence of large chaotic pulsations have a strongly attracting domain of existence, as we tested by degrading the time-dependent solution with the injection of numerical noise and by performing an adiabatic scan for decreasing values of the gain parameter practically down to the laser threshold value. Furthermore, sufficiently large levels of numerical noise (obtained with a uniform random number distribution having a width of about 10% of the output intensity) can perturb the laser steady state, even under low gain conditions, and force the system to jump into the square-wave attractor.

Solutions of the symmetric type have also been found to exist and to evolve stably. In testing this point we have selected, as initial conditions, the stationary values of Eqs. (3.8) as the only nonzero modes for the Fourier expansion (3.1) of the MB variables. When the mode spacing  $\bar{\alpha}_1$  is sufficiently smaller than unity (e.g.,  $\bar{\alpha}_1=0.05$  as in Fig. 11) periodic square-wave solutions for the field amplitude develop with a fundamental frequency given by  $\bar{\alpha}_n$  and a zero average value of the real field  $F(L,t')$  (this is a characteristic feature of the symmetric solutions). By an adiabatic scan of the gain parameter, under conditions (3.11), the symmetric solutions have been found to disap-

pear discontinuously at  $C=C_{\min}$  (see Fig. 3) in agreement with the indications provided by the state equation for  $|f_n|^2$  obtained from the five-mode model. For values of  $\bar{\alpha}_n$  smaller than the right-hand side of Eq. (3.11), the amplitude of the symmetric solution approaches zero as  $C$  approaches  $C_{\text{thr}}$  from above; for  $C < C_{\text{thr}}$ , the only stable state is the stationary solution of the MB equations. In all cases we have seen evidence that the domains of attraction of the symmetric solutions are isolated from the ordinary steady state because of our inability to reach them in other ways than by the assignment of the appropriate initial conditions and that, furthermore, the temporal behavior of the symmetric solution is qualitatively described by the five-mode theory of Sec. III.

#### B. The bad-cavity limit

The relation  $\bar{\kappa}=(|\ln R|/2\pi)\bar{\alpha}_1$  between the intermode spacing and the scaled cavity decay rate puts stringent limitations on both  $R$  and  $\bar{\alpha}_1$  if one wants to ensure that  $\bar{\kappa}$  is sufficiently larger than unity. Thus, for example, with a reflectivity coefficient equal to 0.7, one needs a mode spacing  $\bar{\alpha}_1$  of the order of 25 so that  $\bar{\kappa}\simeq 1.5$ . In this re-

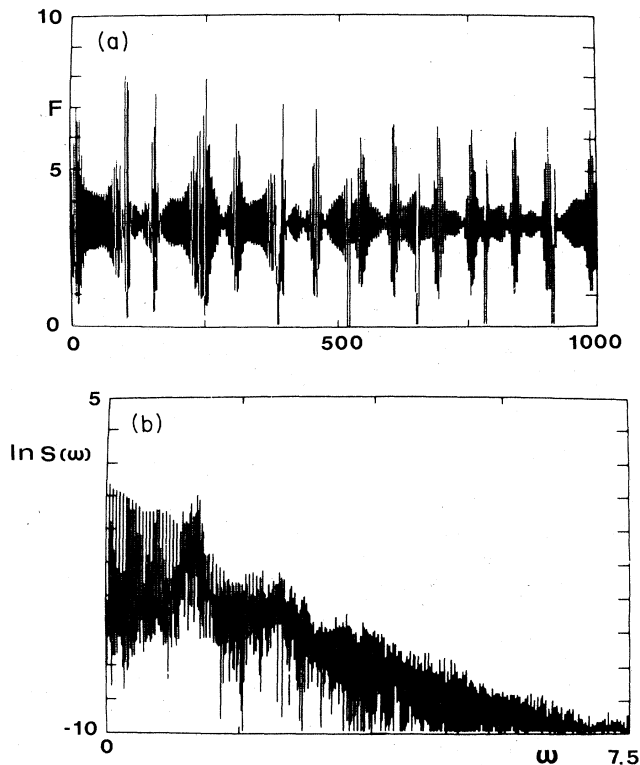


FIG. 9. (a) At a higher gain value than used in Fig. 8, the long-term solution develops sharp irregular bursts which are a symptom of erratic behavior. The parameters used in this simulation are  $\alpha L = 0.62$ ,  $R = 0.95$ , mode spacing  $= 0.05$ ,  $\bar{\gamma} = 0.1$ ,  $\bar{\kappa} = 0.1$ . (b) Power spectrum of the output field on a semilogarithmic scale. Note the broadband structure of the spectrum. The low-frequency, evenly spaced peaks are at a distance  $\bar{\alpha}_1 = 0.05$  from one another.

gime the interaction of the central mode, which can now become unstable, and the nearest sidebands may be quite weak. It is then reasonable to inquire into the ability of the single-mode approximation to provide a good quantitative description of the unstable dynamics of the central mode.

Two interesting facts emerge on exploring this issue: First, for sufficiently small values of  $\bar{\gamma}$  the unstable central mode does not display chaotic oscillations beyond the self-pulsing threshold, but instead displays periodic pulsations with a periodicity that depends on  $\bar{\gamma}$ , and second, even for rather large mode spacing,  $\bar{\alpha}_1$ , the agreement between the single-mode approximation and the exact solution of the MB equations, is rather poor, away from the mean-field limit (Fig. 12). Thus, the single-mode approximation is questionable in general, even if the nearest sidebands are very far from the central mode, and becomes acceptable only if  $R$  approaches unity and if  $\alpha L$  is sufficiently small. The reason for this discrepancy can easily be traced to the spatial dependence of the atomic variables, away from the mean-field limit [see Eqs. (2.7) and (2.4)].

The appearance of regular, instead of chaotic, pulsations in the single-mode model for small values of  $\bar{\gamma}$  is

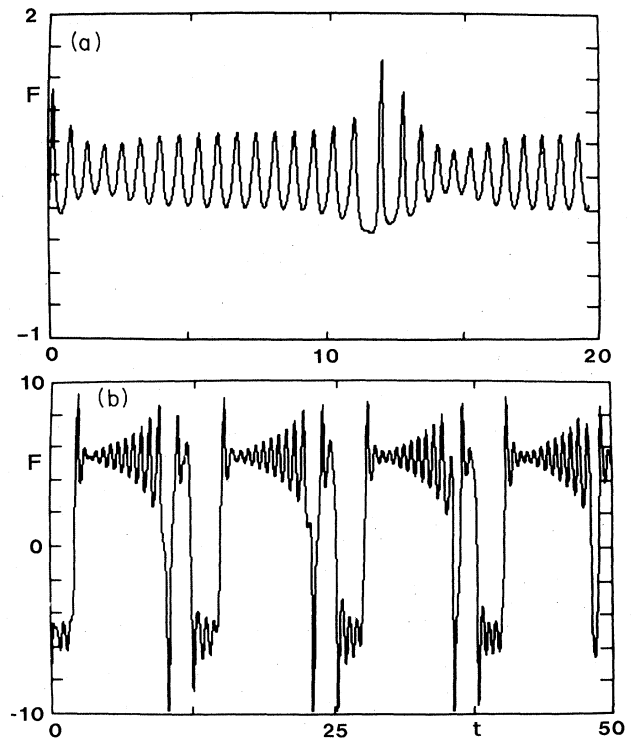


FIG. 10. (a) For sufficiently high gain values, the transient oscillation develops a pattern which is reminiscent of intermittency phenomena. The parameters used in this simulation are  $\bar{\alpha}L = 1.54$ ,  $R = 0.95$ , mode spacing  $= 0.5$ ,  $\bar{\gamma} = 2$ ,  $\bar{\kappa} = 0.05$ . (b) The long-term solution eventually develops a square-wave shape.

rather surprising and will be the subject of a subsequent separate investigation.

## VI. CONCLUSIONS AND OVERVIEW

This investigation on the behavior of a multimode laser was stimulated by the discovery of unstable pulsations in a ring dye laser system by Hillman *et al.*<sup>9</sup> We have stressed in the Introduction and reviewed in greater depth in Sec. V that we are still very far from a satisfactory understanding of the origin of this instability. Thus, while the MB equations for a multimode laser give clear

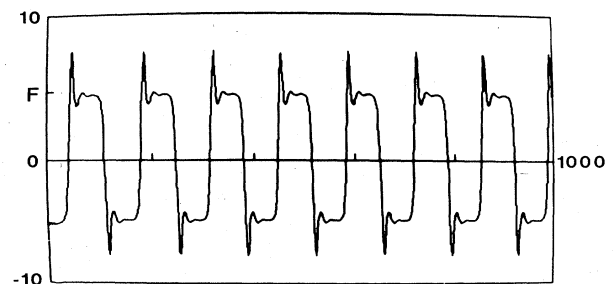


FIG. 11. Example of a symmetric square-wave-like solution generated from the initial conditions given by Eqs. (3.1); the parameters used in this simulation are  $\alpha L = 0.1$ ,  $R = 0.95$ , mode spacing  $= 0.05$ ,  $\bar{\gamma} = 0.1$ ,  $\bar{\kappa} = 0.1$ .

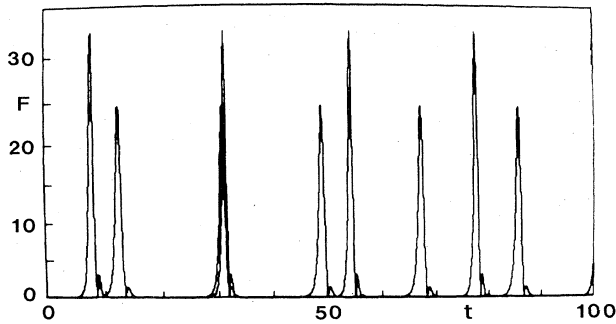


FIG. 12. The solution of the MB equation and of the single-mode approximation (taller spikes) are overlapped in this simulation corresponding to  $\alpha L = 15$ ,  $R = 0.7$ , mode spacing = 50,  $\tilde{\gamma} = 0.01$ ,  $\tilde{\kappa} = 4$ . The two regular trains of pulsations differ both in amplitude and frequency.

evidence for a much richer and complicated behavior than anticipated, no single set of operating parameters and conditions has yielded solutions that match all the key experimental signatures of the effect. These are probably best summarized as follows.

(1) The instability threshold is only slightly higher than the ordinary laser threshold.

(2) The instability is accompanied by a discontinuous increase of the average output power.

(3) A gain scan displays hysteretic behavior of the output intensity; this suggests the presence of coexisting domains of attraction.

(4) Above the instability threshold, the resonant laser mode is suddenly quenched and the output power is shared apparently in an even way between two symmetric sidebands which emerge abruptly with a finite spectral separation.

(5) The spacing between the excited sidebands is a monotonically increasing function of the circulating cavity field, i.e., it depends on the Rabi frequency of the transition. Thus, a rate equation analysis of this problem is not appropriate.

(6) The experimental setting is such that  $\tilde{\alpha}_1 \ll 1$ , i.e., a large number of cavity modes are comprised within the unsaturated atomic line profile.

With reference to our own simulations, the following comments can be made.

(1) According to the linear stability analysis, unstable sidebands emerge symmetrically at a distance from line center which is a monotonically increasing function of the Rabi frequency. This is true both within and outside the mean-field limit. However, the threshold gain for the emergence of this type of instability is several times larger than that required for laser action. Thus, our time-dependent solutions, in the case  $\tilde{\alpha}_1 \ll 1$ , reveal the qualitatively correct spacing between the excited sidebands, but large gain values are required to produce this effect.

(2) The excitation of the sidebands produces a competition between the resonant laser mode and the nonresonant spectral lines; the central mode, however, is never quenched, according to the numerical solutions.

(3) Noise injection into the model creates solutions with a much smaller average power at the resonant frequency

than at the sidebands; still, the resonant mode is not fully quenched and, in any case, the fundamental frequency of the oscillating solution is now close to the intermode spacing  $\tilde{\alpha}_1$  (and, thus, is independent of the Rabi frequency).

(4) Discontinuous behavior has been observed with symmetric solutions. However, the connection between these solutions and the observed experimental features is tenuous. The excitation of symmetric solutions requires rather special initial conditions, and the pulsation frequency is fixed and independent of the Rabi frequency. It is interesting, on the other hand, that at least in principle an infinite number of such solutions exist and that all of them are consistent with a zero amplitude of the resonant mode.

(5) In the bad-cavity limit, a situation which does not relate to the experiments of Ref. 9, we have observed periodic and chaotic solutions of the single-mode Lorenz-type equations. The appearance of periodic solutions is confined to sufficiently low values of  $\tilde{\gamma}$  apart from the usual windows in chaos. A comparison between the solution of the exact MB equations and the single-mode model reveals good quantitative agreement only in the mean-field limit. This result should serve as a warning against an uncritical use of modal expansions. On the other hand, precise criteria for the validity of the truncated modal equations are still lacking and in need of further investigations.

#### ACKNOWLEDGMENTS

We are grateful to Dr. P. Mandel for many stimulating conversations on various topics of this research and to Dr. C. Stroud and Dr. L. Hillman for extensive discussions related to their experiment. We are especially thankful to Mr. H. Sadiqy for his assistance with many of the numerical computations. This work was partially supported by a contract of the U.S. Army Research Office (Durham, NC) and by a travel grant extended to us by the NATO (North Atlantic Treaty Organization) Collaborative Research Program. Additional support was provided by the U.S. National Science Foundation, the Alfred P. Sloan Foundation, and the Italian National Research Council (Consiglio Nazionale delle Ricerche). This research has been carried out in the framework of an operation launched by the Commission of the European Community under the experimental-phase European Community Stimulation Action.

#### APPENDIX: DERIVATION OF EQS. (4.9)

The purpose of this appendix is to sketch the derivation of the state equation for the symmetric five-mode model discussed in Sec. IV. The starting point of this analysis is the set of equations (4.8). We seek steady-state solutions of the form

$$f_{\bar{n}} = \tilde{f}_{\bar{n}} e^{-i\nu t}, \quad p_{\bar{n}} = \tilde{p}_{\bar{n}} e^{-i\nu t}, \quad (\text{A1})$$

$$d_0 = \tilde{d}_0, \quad d_{2\bar{n}} = \tilde{d}_{2\bar{n}} e^{-2i\nu t},$$

where  $\nu$  is the unknown frequency of oscillation of the sideband  $f_{\bar{n}}$  measured relative to the center of the atomic line. With the help of Eqs. (A1), Eqs. (4.8) take the form

$$-i\nu_{\perp}\tilde{f}_{\bar{n}} = -i\tilde{\alpha}_{\bar{n}}\tilde{f}_{\bar{n}} - \tilde{\kappa}(\tilde{f}_{\bar{n}} + 2C\tilde{p}_{\bar{n}}), \quad (\text{A2a})$$

$$-i\nu_{\perp}\tilde{p}_{\bar{n}} = \tilde{f}_{\bar{n}}\tilde{d}_0 + \tilde{f}_{\bar{n}}^*\tilde{d}_{2\bar{n}} - \tilde{p}_{\bar{n}}, \quad (\text{A2b})$$

$$0 = \tilde{f}_{\bar{n}}\tilde{p}_{\bar{n}}^* + \tilde{f}_{\bar{n}}^*\tilde{p}_{\bar{n}} + d_0 + 1, \quad (\text{A2c})$$

$$2i\nu_{\parallel}\tilde{d}_{2\bar{n}} = \tilde{f}_{\bar{n}}\tilde{p}_{\bar{n}} + \tilde{d}_{2\bar{n}}, \quad (\text{A2d})$$

where  $\nu_{\perp} \equiv v/\gamma_{\perp}$  and  $\nu_{\parallel} = v/\gamma_{\parallel}$ . A convenient strategy to solve the algebraic system of equations (A2) is to solve for  $p_{\bar{n}}$  from Eq. (A2b),

$$\tilde{p}_{\bar{n}} = \frac{1}{1-i\nu_{\perp}}(\tilde{f}_{\bar{n}}\tilde{d}_0 + \tilde{f}_{\bar{n}}^*\tilde{d}_{2\bar{n}}), \quad (\text{A3})$$

and to substitute this result into Eqs. (A2c) and (A2d). These can now be solved for  $\tilde{d}_0$  and  $\tilde{d}_{2\bar{n}}$  with the result

$$\tilde{d}_0 = -A/B, \quad (\text{A4})$$

$$\tilde{d}_{2\bar{n}} = \frac{\tilde{f}_{\bar{n}}^2}{(1-2i\nu_{\parallel})(1-i\nu_{\perp}) + |\tilde{f}_{\bar{n}}|^2} \frac{A}{B}, \quad (\text{A5})$$

where

$$A = (1-2\nu_{\perp}\nu_{\parallel} + |\tilde{f}_{\bar{n}}|^2)^2 + (\nu_{\perp} + 2\nu_{\parallel})^2 \quad (\text{A6})$$

and

$$B = 3|\tilde{f}_{\bar{n}}|^4 + 4|\tilde{f}_{\bar{n}}|^2(1-\nu_{\perp}\nu_{\parallel} + 2\nu_{\parallel}^2) + (1+\nu_{\perp}^2)(1+4\nu_{\parallel}^2). \quad (\text{A7})$$

Equations (A4), (A5), and (A3) lead to

$$\tilde{p}_{\bar{n}} = -\frac{A}{B} \frac{\tilde{f}_{\bar{n}}(1-2i\nu_{\parallel})}{(1-2i\nu_{\parallel})(1-i\nu_{\perp}) + |\tilde{f}_{\bar{n}}|^2}. \quad (\text{A8})$$

If we now substitute Eq. (A8) into Eq. (A2a) and separate the real and imaginary parts, the required result follows.

<sup>1</sup>For a recent extensive review of this problem, see, for example, N. B. Abraham, L. A. Lugiato, and L. M. Narducci, *J. Opt. Soc. Am. B* **2**, 7 (1985).

<sup>2</sup>The earliest stability studies for homogeneously broadened laser systems appeared to have been carried out by A. V. Uspenskii, *Radio Eng. Electron. Phys. (USSR)* **8**, 1145 (1963); **9**, 605 (1964); V. V. Korobkin and A. V. Uspenskii, *Zh. Eksp. Teor. Fiz.* **45**, 1003 (1963) [*Sov. Phys.—JETP* **18**, 693 (1964)]; A. Z. Grazyuk and A. N. Oraevskii, in *Quantum Electronics and Coherent Light*, edited by P. A. Miles (Academic, New York, 1964), p. 192; *Radio Eng. Electron. Phys. (USSR)* **9**, 424 (1964); H. Haken, *Z. Phys.* **190**, 327 (1966); H. Risken, C. Schmidt, and W. Weidlich, *Z. Phys.* **194**, 337 (1966).

<sup>3</sup>Unstable behavior in maser systems was investigated by K. Y. Khaldre and R. V. Khokhlov, *Izv. Vyssh. Uchebn. Zaved. Radiofiz.* **1**, 60 (1958); see also A. N. Oraevskii, *Radio Eng. Electron. Phys. (USSR)* **4**, 718 (1959).

<sup>4</sup>(a) R. Graham and H. Haken, *Z. Phys.* **213**, 420 (1968); (b) H. Risken and K. Nummedal, *J. Appl. Phys.* **39**, 4662 (1968).

<sup>5</sup>H. Haken, *Phys. Lett.* **53A**, 77 (1975).

<sup>6</sup>E. N. Lorenz, *J. Atmos. Sci.* **20**, 130 (1963). For a detailed account of the Lorenz model, see C. Sparrow, *The Lorenz Equations: Bifurcations, Chaos, and Strange Attractors*, Vol. 41 of *Applied Mathematical Sciences* (Springer, New York,

1982).

<sup>7</sup>H. Haken and H. Ohno, *Opt. Commun.* **16**, 205 (1976); H. Ohno and H. Haken, *Phys. Lett.* **59A**, 261 (1976); H. Haken and H. Ohno, *Opt. Commun.* **26**, 117 (1978).

<sup>8</sup>For a comprehensive review of this problem in the broader context of synergetics, see H. Haken, *Synergetics: An Introduction*, 3rd ed., Vol. 1 of *Springer Series in Synergetics* (Springer, New York, 1983); *Advanced Synergetics*, Vol. 20 of *Springer Series in Synergetics* (Springer, New York, 1983).

<sup>9</sup>L. W. Hillman, J. Krasinski, R. B. Boyd, and C. R. Stroud, Jr., *Phys. Rev. Lett.* **52**, 1605 (1984).

<sup>10</sup>This assumption was formalized and made rigorous (mean-field limit) with the proof that the commonly used modal expansion for passive (and, implicitly, active) optical systems in this limit could be derived from the standard MB equations for two-level atoms in a unidirectional ring cavity. See, for example, L. A. Lugiato, in *Progress in Optics, Vol. XXI*, edited by E. Wolf (North-Holland, Amsterdam, 1984), p. 71.

<sup>11</sup>V. Benza and L. A. Lugiato, *Z. Phys. B* **35**, 383 (1979).

<sup>12</sup>C. Sparrow, Ref. 6.

<sup>13</sup>J. B. Hamblen and M. Sargent III, *Phys. Rev. A* **13**, 784 (1976); **13**, 797 (1976).

<sup>14</sup>H. J. Carmichael, *Phys. Rev. A* **28**, 480 (1983).